

Kinetic Studies of (μ -Oxo)(μ -carboxylato)bis{[tris(2-pyridylmethyl)amine]chromium(III)} Dimer Acid and Base Hydrolysis Reactions

Thomas F. Tekut and Robert A. Holwerda*

Department of Chemistry and Biochemistry, Texas Tech University, Lubbock, Texas 79409

Received May 6, 1994[Ⓢ]

Kinetic studies of [(tmpa)Cr(μ -O)(μ -RCO₂)Cr(tmpa)]³⁺ aquation and hydroxide-assisted hydrolysis reactions 1 and 2 are reported (tmpa = tris(2-pyridylmethyl)amine; R = H, CH₃, CH₂Cl, CHCl₂, C(CH₃)₃, CPh₃, 1-adamantyl, Ph-4-X (X = H, OH, NMe₂, OCH₃, CH₃, CF₃, NO₂, F, Cl)): [(tmpa)Cr(μ -O)(μ -RCO₂)Cr(tmpa)]³⁺ + H₂O → [(tmpa)Cr(μ -OH)₂Cr(tmpa)]⁴⁺ + RCO₂⁻ (1); [(tmpa)Cr(μ -O)(μ -RCO₂)Cr(tmpa)]³⁺ + 2OH⁻ + H₂O → 2[Cr(tmpa)(OH)₂]⁺ + RCO₂⁻ (2). A linear Hammett plot of acid-independent aquation rate constants (k_{aq}) gives $\rho = +0.30$, while the corresponding plot of $\log(k_{aq})$ vs $-pK_a(\text{RCOOH})$ for R = H, CH₃, CH₂Cl and CHCl₂ complexes exhibits a slope of +0.10; reactivities of carboxylate-bridged complexes with sterically-demanding R groups (CPh₃, C(CH₃)₃, 1-adamantyl) are smaller than anticipated on the basis of RCO₂⁻ basicity alone. For R = H, CH₃, CPh₃, and Ph at 60 °C, and $I = 0.1$ M, $k_{aq} = 1.52 \times 10^{-3} \text{ s}^{-1}$ ($\Delta H^\ddagger = 83 \text{ kJ mol}^{-1}$, $\Delta S^\ddagger = -50 \text{ J mol}^{-1} \text{ K}^{-1}$); $1.08 \times 10^{-3} \text{ s}^{-1}$ ($\Delta H^\ddagger = 77 \text{ kJ mol}^{-1}$, $\Delta S^\ddagger = -71 \text{ J mol}^{-1} \text{ K}^{-1}$); $3.3 \times 10^{-4} \text{ s}^{-1}$ ($\Delta H^\ddagger = 96 \text{ kJ mol}^{-1}$, $\Delta S^\ddagger = -25 \text{ J mol}^{-1} \text{ K}^{-1}$), and $1.64 \times 10^{-3} \text{ s}^{-1}$ ($\Delta H^\ddagger = 80 \text{ kJ mol}^{-1}$, $\Delta S^\ddagger = -59 \text{ J mol}^{-1} \text{ K}^{-1}$), respectively. The proposed aquation mechanism features rate-limiting bridging carboxylate ring-opening to give [(RCO₂)tmpa-Cr(μ -O)Cr(tmpa)(H₂O)]³⁺ as a short-lived intermediate. For base-assisted hydrolysis at 60 °C and $I = 1.0$ M, observed pseudo-first-order rate constants follow the relationship $k_{obsd} = k_o + k_{OH}[\text{OH}^-]$ when R = H ($k_o = 2.8 \times 10^{-3} \text{ s}^{-1}$, $\Delta H^\ddagger = 83 \text{ kJ mol}^{-1}$, $\Delta S^\ddagger = -46 \text{ J mol}^{-1} \text{ K}^{-1}$; $k_{OH} = 6.84 \times 10^{-2} \text{ M}^{-1} \text{ s}^{-1}$, $\Delta H^\ddagger = 86 \text{ kJ mol}^{-1}$, $\Delta S^\ddagger = -8 \text{ J mol}^{-1} \text{ K}^{-1}$). All other [(tmpa)₂Cr₂(μ -O)(μ -RCO₂)]³⁺ species exhibit rate saturation described by $k_{obsd} = k_o + k_b Q_p[\text{OH}^-]/(1 + Q_p[\text{OH}^-])$, where the minor k_o term typically is not resolved at 60 °C; for R = CH₃, $k_b = 6.2 \times 10^{-3} \text{ s}^{-1}$ ($\Delta H^\ddagger = 115 \text{ kJ mol}^{-1}$, $\Delta S^\ddagger = +59 \text{ J mol}^{-1} \text{ K}^{-1}$) and $Q_p = 1.5 \times 10^2 \text{ M}^{-1}$ ($\Delta H^\circ = +65 \text{ kJ mol}^{-1}$, $\Delta S^\circ = +238 \text{ J mol}^{-1} \text{ K}^{-1}$). The proposed base hydrolysis mechanism for [(tmpa)₂Cr₂(μ -O)(μ -RCO₂)]³⁺ (R ≠ H) requires preequilibrium displacement of a tmpa pyridyl arm by OH⁻, followed by rate-limiting ring-opening of the bridging RCO₂⁻ ligand assisted by the solvent or migratory intracomplex nucleophilic attack from the hydroxide ligand.

Introduction

In the course of examining electronic structure–reactivity relationships in oxo-bridged Cr(III) dimers,^{1–6} we have studied bridging and nonbridging ligand hydrolysis reactions in acidic and basic media.^{7–10} For dimers in the class [(tmpa)Cr(μ -O)(μ -RCO₂)Cr(tmpa)]³⁺, inductive and steric effects of the carboxylate substituent have a pronounced effect on oxo bridge basicity and the singlet-triplet energy gap, evaluated from magnetic susceptibility measurements (tmpa = tris(2-pyridylmethyl)amine).^{4,5} Thus, pK_a values for [(tmpa)Cr(μ -OH)(4-X-PhCO₂)Cr(tmpa)]⁴⁺ complexes correlate linearly with Hammett σ_p substituent constants, while steric crowding associated with trimethylacetato and 1-adamantanecarboxylato bridging ligands causes μ -OH⁻ acidities to rise above expectations from inductive considerations alone.⁵ A striking feature of all oxo-bridged dimers in the (tmpa)Cr(III) class is the linear free energy relationship between the Cr(III,IV/III,III) half-wave reduction

potentials and pK_a (Cr(μ -OH)Cr), owing to cooperativity among the oxo bridge, bridging, and nonbridging substituents with regard to π -donation toward Cr(III).^{3,5} All members of the [(tmpa)Cr(μ -O)(μ -RCO₂)Cr(tmpa)]³⁺ family are believed to have the structure reported for the acetato complex, in which one tmpa apical N atom is trans to the oxo bridge while the other is trans to a carboxylate O atom.⁴

A kinetic study of [(en)₂Cr(μ -OH)(μ -CF₃CO₂)Cr(en)]⁴⁺ hydrolysis showed that the reaction proceeds through two distinct phases, acid-independent ($k_1 = 5.4 \times 10^{-3} \text{ s}^{-1}$, 25 °C) or hydroxide-assisted ring-opening of the trifluoroacetate bridging ligand ($k_2 = 4.8 \times 10^3 \text{ M}^{-1} \text{ s}^{-1}$, 25 °C), followed by facile loss of CF₃CO₂⁻ to afford [(OH)(en)₂Cr(μ -OH)Cr(en)₂(OH)]³⁺ or [(en)₂Cr(OH)₂Cr(en)]⁴⁺ as the ultimate product.¹¹ We report here a mechanistic investigation of the corresponding hydrolysis reactions of [(tmpa)Cr(μ -O)(μ -RCO₂)Cr(tmpa)]³⁺ dimers in weakly acidic and basic media, where R = H, CH₃, CH₂Cl, CHCl₂, C(CH₃)₃, CPh₃, 1-adamantyl, and Ph-4-X (X = H, OH, NMe₂, OCH₃, CH₃, CF₃, NO₂, F, Cl). The bridging OH group may be ionized only in strongly basic solutions for the [Cr₂(en)₄(μ -OH)(μ -RCO₂)]⁴⁺ complexes,^{11,12} in contrast to the [(tmpa)Cr(μ -OH)(μ -RCO₂)Cr(tmpa)]⁴⁺ system for which μ -OH⁻ pK_a 's range from 0.46 to 2.21.^{4,5} Thus, we have been able to specifically determine the hydrolytic reactivities of the oxo-bridged dimers under both weakly acidic and strongly basic conditions, according to reactions 1 and 2, respectively. As has been described previously for the base hydrolysis reactions of [(tmpa)Cr(O)₂Cr(tmpa)]²⁺ and [Cr(tmpa)L₂O₂⁺ (L = NCS⁻,

* Abstract published in *Advance ACS Abstracts*, October 1, 1994.

- (1) Gafford, B. G.; O'Rear, C.; Zhang, J. H.; O'Connor, C. J.; Holwerda, R. A. *Inorg. Chem.* **1989**, *28*, 1720.
- (2) Holwerda, R. A.; Tekut, T. F.; Gafford, B. G.; Zhang, J. H.; O'Connor, C. J. *J. Chem. Soc., Dalton Trans.* **1991**, 1051.
- (3) Tekut, T. F.; O'Connor, C. J.; Holwerda, R. A. *Inorg. Chem.* **1993**, *32*, 324.
- (4) Gafford, B. G.; Marsh, R. E.; Schaefer, W. P.; Zhang, J. H.; O'Connor, C. J.; Holwerda, R. A. *Inorg. Chem.* **1990**, *29*, 4652.
- (5) Tekut, T. F.; O'Connor, C. J.; Holwerda, R. A. *Inorg. Chim. Acta* **1993**, *214*, 145.
- (6) Holwerda, R. A. *Polyhedron* **1994**, *13*, 737.
- (7) Gafford, B. G.; Holwerda, R. A. *Inorg. Chem.* **1988**, *27*, 210.
- (8) Gafford, B. G.; Holwerda, R. A. *Inorg. Chem.* **1989**, *28*, 60.
- (9) Gafford, B. G.; Holwerda, R. A. *Inorg. Chem.* **1990**, *29*, 233.
- (10) Tekut, T. F.; Holwerda, R. A. *Inorg. Chem.* **1993**, *32*, 3196.

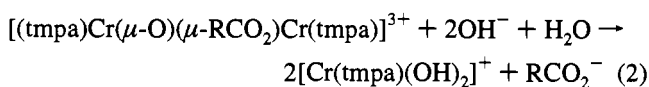
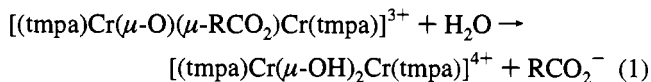
(11) Springborg, J. *Acta Chem. Scand.* **1992**, *46*, 1047.

(12) Springborg, J.; Toftlund, H. *Acta Chem. Scand., Ser. A* **1979**, *33*, 31.

Table 1. Rate Parameters for [(tmpa)Cr(μ -O)(μ -RCO₂)Cr(tmpa)]³⁺ Hydrolysis Reactions^a

R	temp, °C	10 ³ k _o , s ⁻¹	10 ³ k _b , s ⁻¹	10 ⁻² Q _p , M ⁻¹	10 ² k _{OH} , M ⁻¹ s ⁻¹	10 ³ k _{aq} , s ⁻¹	σ_p
H	60.0	2.8(0.4)			6.84(0.08)	1.52	
	50.0	1.0(0.1)			2.77(0.05)	0.592	
	40.0	0.39(0.02)			0.886(0.005)	0.210	
CH ₃	60.0		6.2(0.1)	1.5(0.1)	93	1.08	
	50.0	0.53(0.14)	1.7(0.1)	0.65(0.12)	11	0.439	
	40.0	0.32(0.04)	0.40(0.03)	0.34(0.09)	1.4	0.172	
	30.0	0.19(0.01)	0.092(0.002)	0.14(0.01)	0.17		
CH ₂ Cl	60.0		8.6(0.1)	1.1(0.1)	95	1.40	
CHCl ₂	60.0	4.3(0.3)	16.0(0.6)	0.07(0.01)	11	2.55	
CCl ₃ ^b	60.0		7.3(0.3)	0.06(0.01)	4.4		
C(CH ₃) ₃	60.0		5.8(0.1)	1.1(0.1)	64	0.466	
C(C ₆ H ₅) ₃	60.0		2.5(0.1)	2.3(0.3)	58	0.33	
	50.0					0.12	
	40.0					0.034	
C ₁₀ H ₁₅ ^c	60.0		6.0(0.1)	0.71(0.05)	43	0.45	
	Ph	60.0		8.4(0.1)	0.88(0.06)	74	1.64
	50.0					0.630	
	40.0					0.242	
Ph-4-OH ^d	60.0	4.1(0.5)	5.4(0.5)	0.05(0.03)	2.7	1.36	-0.37
Ph-4-NMe ₂	60.0		8.5(0.1)	1.2(0.1)	100	0.89	-0.83
Ph-4-OCH ₃	60.0		8.3(0.1)	1.0(0.1)	83	1.47	-0.268
Ph-4-CH ₃	60.0		8.7(0.1)	0.72(0.05)	63	1.47	-0.17
Ph-4-CF ₃	60.0		8.8(0.1)	1.2(0.1)	110	2.48	0.54
Ph-4-NO ₂	60.0		10.5(0.2)	0.79(0.09)	83	2.75	0.778
	50.0					1.06	
	40.0					0.393	
Ph-4-F	60.0		9.2(0.1)	0.87(0.08)	80	1.88	0.062
Ph-4-Cl	60.0		8.8(0.1)	1.1(0.1)	97	2.05	0.227

^a Rate parameters for base hydrolysis defined by the relationships $k_{\text{obsd}} = k_o + k_{\text{OH}}[\text{OH}^-]$ (R = H) and $k_{\text{obsd}} = k_o + k_b Q_p / (1 + Q_p[\text{OH}^-])$ (all other R groups); $I = 1.0$ M. For R \neq H, k_{OH} is calculated as $k_b Q_p$. Hydrogen ion-independent rate constant for acid hydrolysis designated as k_{aq} ; $I = 0.1$ M. Uncertainty in k_{aq} estimated at $\pm 3\%$. Standard deviations shown in parentheses. ^b [(OH)(tmpa)Cr(μ -O)Cr(tmpa)(CCl₃CO₂)]²⁺ complex; carboxylate group is not bridging. ^c R = 1-adamantyl group. ^d Base hydrolysis parameters correspond to the Ph-4-O⁻ complex.



NCO⁻, CN⁻), the intermediate [Cr(tmpa)(OH)]₂O²⁺ is formed in the base hydrolyses of carboxylate-bridged complexes, such that the kinetics reported describes loss of the μ -RCO₂⁻ ligand rather than oxo-bridge cleavage.

Experimental Section

Dinuclear complexes of the type [(tmpa)Cr(μ -O)(μ -RCO₂)Cr(tmpa)]-(ClO₄)₃ and [(OH)(tmpa)Cr(μ -O)Cr(tmpa)(CCl₃CO₂)](ClO₄)₂ were available from laboratory stock.^{4,5} Methods used to acquire electronic spectra, perform cation exchange chromatography (SP-Sephadex-C-25 resin) and identify [Cr(tmpa)(OH)]₂O²⁺ as an intermediate have been described.⁸⁻¹⁰ Kinetic measurements (Shimadzu UV-260 spectrophotometer, $\lambda = 336$ nm) were carried out on samples in thermostated (± 0.2 °C) 1 cm path length cells. Runs were initiated by injecting 0.1 mL of a dimer stock solution prepared with CH₃CN into 3.0 mL of the aqueous reaction medium; initial dimer concentrations were 0.2–0.3 mM. Solutions were prepared from distilled water and maintained at ionic strengths of 0.1 M (acid studies) or 1.0 M (base studies) with NaNO₃. Acidic solutions in the pH range 3–4 were prepared by dilution of standard HNO₃. Weakly acidic solutions were buffered with 1 mM MES; [H⁺] values were determined from activity-corrected pH readings.¹³ Base hydrolysis studies were performed with standardized NaOH/NaNO₃ mixtures. Reported acid hydrolysis rate constants (k_{aq}) and pseudo-first-order base hydrolysis rate constants (k_{obsd}) were derived from the least-squares slopes of $\ln|A_t - A_\infty|$ vs time plots that were linear over $\geq 90\%$ of the overall absorbance change; most values are the mean of three independent determinations.

Results and Discussion

As compared with trifluoroacetate hydrolysis in [(en)₂Cr(OH)-(CF₃CO₂)Cr(en)]⁴⁺,¹¹ the transformation of [(tmpa)Cr(μ -O)(μ -RCO₂)Cr(tmpa)]³⁺ to [Cr(tmpa)(OH)]₂⁴⁺ in acidic solution is very slow at 25 °C. For this reason, kinetics studies were performed in the 40–60 °C interval. Time course 300–500 nm spectra of reaction mixtures at 60 °C showed that no appreciable concentration of a hydrolysis intermediate such as [(H₂O)(tmpa)-Cr(O)Cr(tmpa)(RCO₂)]³⁺ builds up during the reaction, in contrast to the equilibrium between [(en)₂Cr(OH)(CF₃CO₂)Cr(en)]⁴⁺ and [(H₂O)(en)₂Cr(OH)Cr(en)₂(CF₃CO₂)]⁴⁺ ($K_1 = 0.39$).¹¹ Furthermore, chromatography of quenched reaction mixtures (R = CH₃) showed only two bands, assigned by their spectra to reactant and product species.

A survey of bridging carboxylate aquation rate constants at pH 6.0, 60 °C is given in Table 1, along with temperature dependence findings for R = H, CH₃, C(CH₃)₃, and Ph. A pH variation study in the 3.0–6.4 interval for R = H, CH₃, and Ph (Table 2) showed that the acid hydrolysis rate is independent of [H⁺], to within experimental uncertainty, under conditions where the oxo- rather than the hydroxo-bridged dimer is the dominant reactant species. For R = CH₃, rate measurements at three different reactant absorption maxima (336, 372, 419 nm) and the product λ_{max} of 540 nm (Table 2) gave identical results. On this basis, the simple rate law of eq 3 is justified. An acid hydrolysis rate constant could not be determined for [(OH)(tmpa)Cr(μ -O)Cr(tmpa)(CCl₃CO₂)]²⁺ since $pK_a(\text{Cr}(\mu\text{-OH})\text{Cr}) = 5.95$.⁵

$$k_{\text{obsd}} = k_{\text{aq}} \quad (3)$$

The base hydrolysis reactivities of [(OH)(tmpa)Cr(μ -O)Cr(tmpa)(CCl₃CO₂)]²⁺ and 16 [(tmpa)Cr(μ -O)(μ -RCO₂)Cr(tmpa)]³⁺ complexes were determined at 60 °C as a function of [OH⁻] in

Table 2. Acid Hydrolysis Rate Data for [(tmpa)Cr(μ -O)(μ -RCO₂)Cr(tmpa)]³⁺ Dimers^a

R	[H ⁺], M	10 ³ k _{aq} , s ⁻¹
H	1.02 × 10 ⁻⁶	1.52
	1.12 × 10 ⁻⁵	1.49
	1.00 × 10 ⁻⁴	1.51
	1.00 × 10 ⁻³	1.62
CH ₃	4.37 × 10 ⁻⁷	1.06
	1.02 × 10 ⁻⁶	1.08
	1.02 × 10 ⁻⁶	1.09 ^b
	1.02 × 10 ⁻⁶	1.05 ^c
	1.02 × 10 ⁻⁶	1.08 ^d
	4.47 × 10 ⁻⁶	1.06
	1.12 × 10 ⁻⁵	1.06
	1.00 × 10 ⁻⁴	1.06
	1.00 × 10 ⁻³	1.05
Ph	1.02 × 10 ⁻⁶	1.64
	1.12 × 10 ⁻⁵	1.63
	1.00 × 10 ⁻⁴	1.66

^a 60.0 °C, *I* = 0.1 M (NaNO₃); reaction monitored at 336 nm unless otherwise stated. Uncertainty in k_{aq} estimated at ±3%. ^b Reaction monitored at 372 nm. ^c Reaction monitored at 419 nm. ^d Reaction monitored at 540 nm.

the 0.005–1.0 M range (Table 3). In addition, temperature dependence data were acquired for R = H (Figure 1) and CH₃ (Figure 2). Time course spectra showed that dimers were quantitatively converted to [Cr(tmpa)(OH)₂]⁺ and quenching of reaction mixtures with HNO₃ after one half-life gave [Cr(tmpa)(OH)₂]⁴⁺ and [Cr(tmpa)(H₂O)₂]³⁺ as the sole trapping products, consistent with our previous report that [Cr(tmpa)(OH)₂O]²⁺ is an intermediate in the base hydrolysis reactions of both singly- and doubly-bridged (tmpa)CrOcr(tmpa) species.^{8,9} Reported base hydrolysis kinetic parameters pertain specifically to the loss of bridging carboxylate rather than oxo-bridge cleavage since the 336 nm absorbances of intermediate and product species are negligible when compared with those of the [Cr₂(tmpa)₂(μ -O)(μ -RCO₂)]³⁺ reactants.

With R = H, observed rate constants were fit to the two-term rate law of eq 4. Thus, k_{obsd} vs [OH⁻] plots were found to be linear, with small positive intercepts, throughout the entire OH⁻ concentration range and at every temperature. In contrast,

$$k_{\text{obsd}} = k_0 + k_{\text{OH}}[\text{OH}^-] \quad (4)$$

k_{obsd} vs [OH⁻] plots for all other R groups exhibit marked curvature, which we attribute to an intermediate complex mechanism (vide infra) characterized by a precursor formation constant (*Q*_p) and an intermediate complex decay rate constant (*k*_b). Nonlinear least-squares fits (Marquardt algorithm) of k_{obsd} vs [OH⁻] profiles to eq 5 were successful, except that the minor

$$k_{\text{obsd}} = k_0 + k_b Q_p [\text{OH}^-] / (1 + Q_p [\text{OH}^-]) \quad (5)$$

k₀ term was sufficiently large to be quantitatively resolved only in the cases of R = CHCl₂, Ph-4-O⁻, and CH₃ at lower temperatures (30–50 °C). The parameters *k*_b, *Q*_p and *k*_{OH} = *k*_b*Q*_p are summarized in Table 1. Table 4 presents activation (*k*₀, *k*_b, *k*_{aq}) and standard (*Q*_p) enthalpy and entropy changes.

Linear free energy relationships are frequently exploited to define the degree of bond-making to incoming groups or bond-breaking to leaving groups in the substitution reactions of transition metal ions.^{14–23} A linear Hammett plot of rate data

for the displacement of 4-X-benzoato bridging ligands according to reaction 1 (Figure 3) gives $\rho = +0.30 \pm 0.02$ (correlation coefficient = 0.99). The Hammett ρ parameter is slightly temperature-dependent, typically decreasing with increasing *T*.²⁴ In order to make comparisons with ρ values for reactions studied at temperatures lower than 60 °C, we estimate the upper limit of ρ (25 °C) at 0.34 from an equation given by Wells.²⁴ By comparison, the sensitivity of μ -OH⁻ acidity to the inductive characteristics of R ($\rho = -0.81$)⁵ is larger by a factor of 2.7. Analogous plots of log(*k*_{aq}) and p*K*_a(Cr(μ -OH)Cr) vs -p*K*_a(RCOOH) for [(tmpa)Cr(μ -O)(μ -RCO₂)Cr(tmpa)]³⁺ dimers with aliphatic R groups (Figure 4) are markedly nonlinear, indicating that both steric and inductive factors must be considered in describing both the carboxylate hydrolysis mechanism and the μ -OH⁻ ionization process. For comparison purposes only, we show the least-squares lines defined by the four dimers (R = H, CH₃, CH₂Cl, CHCl₂) for which the kinetic (slope = +0.10 ± 0.03, correlation coefficient = 0.94) and ionization constant (slope = -0.48 ± 0.07, correlation coefficient = 0.98) correlations are reasonably linear. Points which fall well below the line in both correlations correspond to bulky substituents, CPh₃, C(CH₃)₃, and 1-adamantyl. Protonation of [(tmpa)Cr(μ -O)(μ -RCO₂)Cr(tmpa)]³⁺ dimers with sterically-demanding R groups evidently is hindered to the extent that substituent repulsions with tmpa pyridyl rings increase as a consequence of the Cr–O–Cr bond angle reduction.

Hydrolysis rates of benzoato ligands from [(tmpa)Cr(μ -O)(μ -{Ph-4-X}CO₂)Cr(tmpa)]³⁺ dimers are less sensitive to substituent inductive effects than is typical of related processes in monomeric complexes. Thus, a LFER between rate and equilibrium constants for L⁻ hydrolysis in [(H₂O)₅CrL]²⁺ complexes has a slope of 0.56 (25 °C, *I* = 1.0 M).¹⁷ Similarly, reaction constants for the base hydrolysis of a carboxylate ligand from *trans*-[Co(en)₂(ArCO₂)₂]⁺ (0.745, 25 °C)²⁰ and the anation of *cis*-[Co(en)₂(H₂O)Cl]²⁺ to give *cis*-[Co(en)₂(ArCO₂)Cl]⁺ (-1.60, 30 °C, 15% EtOH/H₂O)²¹ indicate much larger degrees of metal–carboxylate oxygen bond-breaking or bond-making, respectively, than is the case for reaction 1. A Taft plot of base hydrolysis rate data for [Co(NH₃)₅(RCO₂)]²⁺ complexes^{22,23} is consistent with an activated complex exhibiting substantial Co–O bond-breaking ($\rho = 0.99$, 25 °C, calculated from data given in ref 22). Reaction constants for processes in which carboxylate C–O bond-breaking occurs, i.e. ester hydrolysis, are much larger (>2)²⁴ than any that has been reported for a metal–carboxylate O cleavage reaction.

The proposed aquation mechanism (Figure 5) is similar to that advocated by Springborg for [(en)₂Cr(OH)(CF₃CO₂)Cr(en)₂]⁴⁺ hydrolysis.¹¹ With regard to this mechanistic schematic, we note that the kinetic data do not permit a distinction between initial Cr–O bond breakings *trans* to apical (as shown) or pyridyl N atoms. Possible rate-limiting steps include cleavage of the first (*k*_{aq} = *k*₁; *k*₂/*k*₋₁ ≫ 1) or second (*k*_{aq} = *k*₁*k*₂/*k*₋₁; *k*₂/*k*₋₁ ≪ 1) Cr–O bond to the bridging carboxylate ligand. In view of the small reaction constant for 4-XPhCO₂⁻ leaving groups, the second alternative may be excluded. Carboxylate basicity should have little effect on the rate of a process in which a metal–carboxylate oxygen bond breaks in the rate-limiting step without departure of RCO₂⁻ from the first coordination

(19) Lee, W. K.; Poon, C. K. *Inorg. Chem.* **1974**, 13, 2526.(20) Aprile, F.; Caglioti, V.; Illuminati, G. *J. Inorg. Nucl. Chem.* **1961**, 21, 325.(21) Ghoshal, A.; Siddhanta, S. K. *Indian J. Chem.* **1981**, 20A, 40.(22) Jones, W. E.; Thomas, J. D. R. *J. Chem. Soc. A* **1968**, 1481.(23) Basolo, F.; Bergmann, J. G.; Pearson, R. G. *J. Phys. Chem.* **1952**, 56, 22.(24) Wells, P. R. *Chem. Rev.* **1963**, 63, 171.(14) Haim, A. *Inorg. Chem.* **1970**, 9, 426.(15) Langford, C. H. *Inorg. Chem.* **1965**, 4, 265.(16) Kernohan, J. A.; Endicott, J. F. *Inorg. Chem.* **1970**, 9, 1504.(17) Swaddle, T. W.; Guastalla, G. *Inorg. Chem.* **1968**, 7, 1915.(18) Jones, T. P.; Phillips, J. K. *J. Chem. Soc. A* **1968**, 674.

Table 3. Base Hydrolysis Rate Data for [(tmpa)Cr(μ -O)(μ -RCO₂)Cr(tmpa)]³⁺ Dimers^a

R	temp, °C	[OH ⁻], M	10 ³ k _{obsd} , s ⁻¹	R	temp, °C	[OH ⁻], M	10 ³ k _{obsd} , s ⁻¹
H	60.0	0.01	3.32	C(C ₆ H ₅) ₃	60.0	0.01	1.68
		0.02	4.96			0.02	2.15
		0.05	6.77			0.05	2.30
		0.10	8.63			0.10	2.37
		0.50	36.6			0.50	2.46
	50.0	1.00	71.5	C ₁₀ H ₁₅ ^c	60.0	1.00	2.50
		0.01	1.34			0.01	2.45
		0.02	1.72			0.02	3.66
		0.05	2.41			0.05	4.74
		0.10	3.45			0.10	5.20
	40.0	0.50	14.9	Ph	60.0	0.50	5.76
		0.01	0.430			1.00	6.13
		0.02	0.560			0.01	3.72
		0.05	0.807			0.02	5.58
		0.10	1.34			0.05	6.95
CH ₃	60.0	0.50	4.83	Ph-4-O ^{-d}	60.0	0.10	7.47
		1.00	9.23			0.50	8.18
		0.005	2.71			1.00	8.37
		0.01	3.60			0.02	4.44
		0.02	4.74			0.05	5.53
	50.0	0.05	5.54	Ph-4-NMe ₂	60.0	0.10	5.99
		0.10	5.80			0.50	7.79
		0.50	6.05			1.00	8.85
		1.00	6.17			0.01	4.46
		0.01	1.18			0.02	6.09
	40.0	0.02	1.48	Ph-4-OCH ₃	60.0	0.05	7.24
		0.05	1.77			0.10	7.84
		0.10	2.00			0.50	8.13
		0.50	2.13			1.00	8.56
		1.00	2.17			0.02	5.46
30.0	0.01	0.418	Ph-4-CH ₃	60.0	0.05	7.06	
	0.02	0.482			0.10	7.48	
	0.05	0.579			0.50	8.06	
	0.10	0.619			1.00	8.18	
	0.50	0.683			0.02	5.23	
60.0	1.00	0.722	Ph-4-CF ₃	60.0	0.05	6.77	
	0.01	0.201			0.10	7.47	
	0.02	0.209			0.50	8.44	
	0.05	0.226			1.00	8.73	
	0.10	0.244			0.02	6.08	
60.0	0.50	0.269	Ph-4-NO ₂	60.0	0.05	7.68	
	1.00	0.276			0.10	8.12	
	0.01	4.45			0.50	8.46	
	0.02	5.93			1.00	8.73	
	0.05	7.26			0.01	4.26	
60.0	0.10	7.70	Ph-4-F	60.0	0.02	6.81	
	0.50	8.53			0.05	8.53	
	0.01	5.13			0.10	9.11	
	0.02	6.39			0.50	9.97	
	0.05	8.59			1.00	10.6	
60.0	0.10	10.6	Ph-4-Cl	60.0	0.02	5.69	
	0.50	16.7			0.05	7.70	
	0.01	0.438			0.10	8.31	
	0.02	0.737			0.50	8.84	
	0.05	1.77			1.00	9.10	
60.0	0.10	2.74	C(CH ₃) ₃	60.0	0.02	6.01	
	0.50	5.19			0.05	7.57	
	1.00	6.43			0.10	7.96	
	0.01	3.04			0.50	8.66	
	0.02	4.02			1.00	8.81	
60.0	0.05	4.98					
	0.10	5.32					
	0.50	5.68					
	1.00	5.82					

^a *I* = 1.0 M (NaNO₃); reaction monitored at 336 nm unless otherwise stated. Uncertainty in *k*_{obsd} estimated at ±5%. ^b [(OH)(tmpa)Cr(μ -O)Cr(tmpa)(CCl₃CO₂)]²⁺ complex; carboxylate group is not bridging. ^c R = 1-adamantyl group. ^d Reaction monitored at 400 nm.

sphere. Aquation activation parameters for R = H, CH₃, Ph, and Ph-4-NO₂ are in reasonable agreement with those of the [(en)₂Cr(OH)(CF₃CO₂)Cr(en)₂]⁴⁺ ring-opening reaction (ΔH^\ddagger = 68 kJ mol⁻¹, ΔS^\ddagger = -61 J mol⁻¹ K⁻¹),¹¹ considering the weakening of Cr(III)-O₂CR bonding expected when RCO₂⁻ is the weakly-basic trifluoroacetate ligand. On average, *k*_{aq}

activation enthalpies characteristic of R = H, CH₃, Ph, and Ph-4-NO₂ are larger by about 13 kJ mol⁻¹, but essentially invariant from one R group to another; the average ΔS^\ddagger value for these same four tmpa dimers is -59 J mol⁻¹ K⁻¹.

Our assignment of rate-limiting step is supported by the absence of a long-lived intermediate or biphasic kinetic behavior.

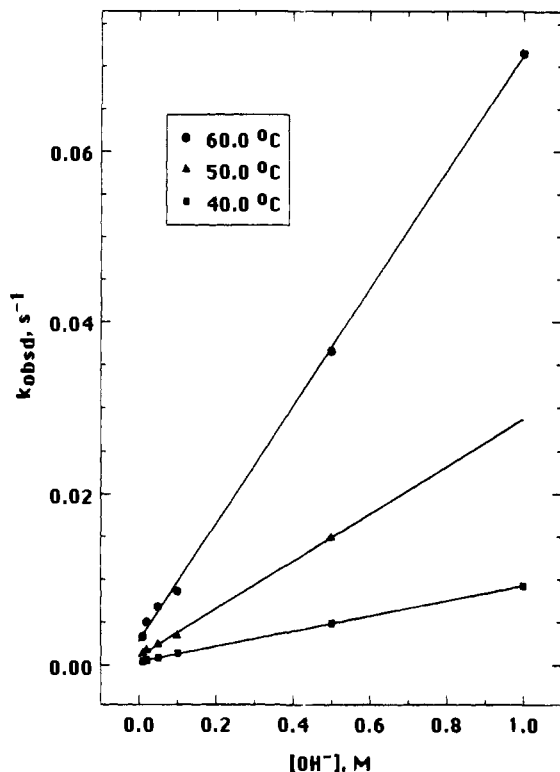


Figure 1. Hydroxide concentration dependence of observed rate constants for the base hydrolysis of $[(\text{tmpa})\text{Cr}(\text{O})(\text{HCO}_2)\text{Cr}(\text{tmpa})]^{3+}$. $I = 1.0 \text{ M}$.

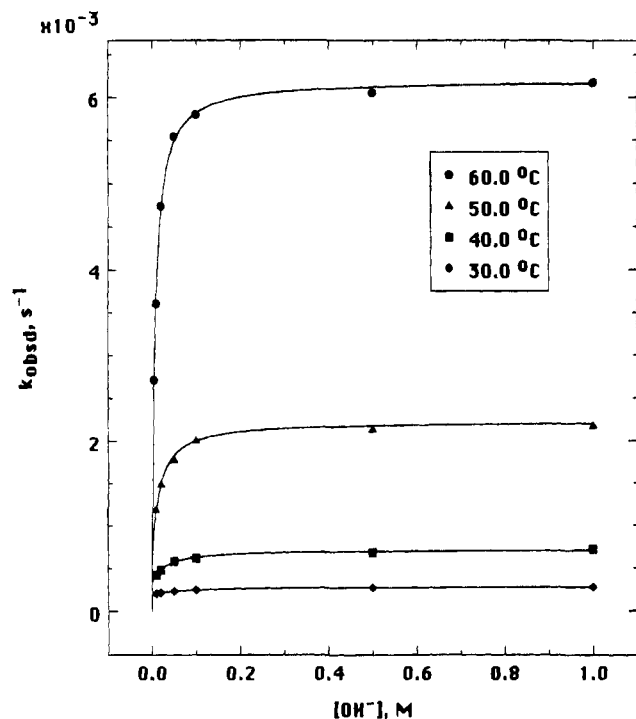


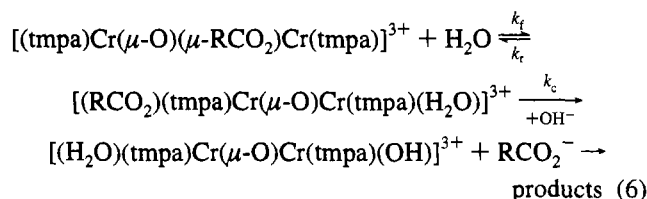
Figure 2. Hydroxide concentration dependence of observed rate constants for the base hydrolysis of $[(\text{tmpa})\text{Cr}(\text{O})(\text{CH}_3\text{CO}_2)\text{Cr}(\text{tmpa})]^{3+}$. $I = 1.0 \text{ M}$.

Severe steric hindrance of the aquation pathway for $R = 1\text{-adamantyl}$, $\text{C}(\text{CH}_3)_3$ and $\text{C}(\text{C}_6\text{H}_5)_3$ is consistent with the proposed mechanism. Thus, bulky substituents are expected to interfere with the approach of an incoming water ligand toward the first coordination sphere of $\text{Cr}(\text{III})$ and steric interactions between the R group and tmpa pyridyl rings will increase with decreasing $\text{CrO}(\text{Cr})$ bond angle in the course of

replacing a $\mu\text{-RCO}_2^-$ ligand with $\mu\text{-OH}^-$; for $[(\text{tmpa})\text{Cr}(\mu\text{-O})(\mu\text{-CH}_3\text{CO}_2)\text{Cr}(\text{tmpa})]^{3+}$ and $[(\text{tmpa})\text{Cr}(\mu\text{-OH})_2\text{Cr}(\text{tmpa})]^{4+}$, the $\text{CrO}(\text{Cr})$ angles are 132 and 101° , respectively.^{4,8} A similar steric argument has been proposed to explain the departure of $R = \text{C}(\text{CH}_3)_3$ from a Taft plot for inner-sphere reductions of $[(\text{NH}_3)_5\text{-Co}(\text{RCO}_2)]^{2+}$ complexes by Cr^{2+} .²⁵ Aquation activation parameters for $R = \text{CPh}_3$ show that rate retardation follows from an increase of 19 kJ mol^{-1} in ΔH^\ddagger relative to the acetate-bridged complex, while ΔS^\ddagger is more favorable by $46 \text{ J mol}^{-1} \text{ K}^{-1}$. A reasonably linear isokinetic relationship between ΔH^\ddagger and ΔS^\ddagger pertains for the aquation reactions of $[(\text{tmpa})\text{Cr}(\mu\text{-O})(\mu\text{-RCO}_2)\text{-Cr}(\text{tmpa})]^{3+}$ complexes; isokinetic temperature = $426 \pm 55 \text{ K}$ (correlation coefficient = 0.98 for five sets of k_{aq} activation parameters). We conclude therefore that the same aquation mechanism pertains for all substituents, with compensating trends in ΔH^\ddagger and ΔS^\ddagger most likely relating to the relative contributions of $\text{Cr}-\text{O}_2\text{CR}$ bond-breaking and $\text{Cr}-\text{OH}_2$ bond-making in the activated complex for the k_1 step.

The finding of rate saturation in k_{obsd} vs $[\text{OH}^-]$ plots for the base hydrolysis reactions of oxo, carboxylato-bridged dimers was not anticipated, considering that the straightforward rate law of eq 4 pertains in the corresponding reactions of $[\text{Cr}(\text{tmpa})(\text{O})]_2^{2+}$, $[\text{Cr}(\text{tmpa})(\text{OH})]_2\text{O}^{2+}$ and $[\text{Cr}(\text{tmpa})\text{L}]_2\text{O}^{2+}$ ($\text{L} = \text{NCO}^-$, CN^-).^{8,9} The two-term saturation rate law of eq 5 was observed previously, however, for the base-induced decomposition of $[\text{Cr}(\text{tmpa})(\text{NCS})]_2\text{O}^{2+}$.⁹ Several mechanistic alternatives must be considered to account for the finding of rate saturation in the reactions of $[(\text{OH})(\text{tmpa})\text{Cr}(\mu\text{-O})\text{Cr}(\text{tmpa})(\text{CCl}_3\text{CO}_2)]^{2+}$ and $[(\text{tmpa})\text{Cr}(\text{O})(\text{RCO}_2)\text{Cr}(\text{tmpa})]^{3+}$ dimers, with the sole exception occurring in the case of the simplest substituent, $R \approx \text{H}$. A strong interaction between OH^- and the LUMO (b_{1u}) orbital of linear²⁶ $[\text{Cr}(\text{tmpa})(\text{NCS})]_2\text{O}^{2+}$ was tentatively proposed⁹ to account for saturation in its base hydrolysis kinetics, but this explanation could not account for the failure of the $\text{L} = \text{NCO}^-$ and CN^- dimers to exhibit similar behavior.

A second base hydrolysis mechanism to be considered features reversible ring-opening of the $\mu\text{-RCO}_2^-$ group, followed by irreversible displacement of the monodentate carboxylate ligand



by OH^- . On this basis, the steady-state parameter counterparts of k_b and Q_p are k_f and k_c/k_r , respectively. Although plausible, this mechanism cannot account for saturation kinetics in the base hydrolysis reaction of $[\text{Cr}(\text{tmpa})(\text{NCS})]_2\text{O}^{2+}$, which lacks a complementary bridging ligand but nevertheless displays Q_p and k_b values with associated enthalpy and entropy changes which resemble those for the acetate-bridged dimer (Table 4). Similarly, $[(\text{OH})(\text{tmpa})\text{Cr}(\mu\text{-O})\text{Cr}(\text{tmpa})(\text{CCl}_3\text{CO}_2)]^{2+}$ should not show saturation behavior on the basis of mechanism 6 and the finding of a smaller saturation rate constant for $R = \text{CCl}_3$ than for $R = \text{CHCl}_2$ is unexpected. A plot of $\log(\text{limiting } k = k_b \text{ or } k_f) \text{ vs } \sigma_p$ exhibits poor linearity (correlation coefficient = 0.70) with a slope (0.05 ± 0.02) which points to a process even less sensitive to the inductive characteristics of Ph-4-X groups

(25) Barrett, M. B.; Swinehart, J. H.; Taube, H. *Inorg. Chem.* **1971**, *10*, 1983.

(26) Gafford, B. G.; Holwerda, R. A.; Schugar, H. J.; Potenza, J. A. *Inorg. Chem.* **1988**, *27*, 1126.

Table 4. Activation Parameters for Acid and Base Hydrolysis Reactions of (tmpa)Cr^{III} Dimers^a

complex	param	$k(25\text{ }^\circ\text{C})$	ΔH^\ddagger	ΔS^\ddagger	ΔH°	ΔS°
[(tmpa)Cr(O) ₂ Cr(tmpa)] ²⁺ ^b	k_o	3.0×10^{-4}	83	-33		
	k_{OH}	5.8×10^{-4}	94	+8		
[Cr(tmpa)(OH)] ₂ O ²⁺ ^c	k_o	4.7×10^{-5}	96	-4		
	k_{OH}	2.7×10^{-5}	117	+59		
[Cr(tmpa)(NCS)] ₂ O ²⁺ ^d	k_o	6.6×10^{-6}	75	-92		
	k_b	1.5×10^{-4}	90	-17		
	Q_p				24	+105
[Cr ₂ (tmpa) ₂ (μ -O)(μ -HCO ₂)] ³⁺	k_{OH}^e	2.5×10^{-3}	114	+88		
	k_o	7.6×10^{-5}	83(4)	-46(12)		
	k_{OH}	1.6×10^{-3}	86(4)	-8(12)		
	k_{aq}	4.1×10^{-5}	83(1)	-50(4)		
[Cr ₂ (tmpa) ₂ (μ -O)(μ -CH ₃ CO ₂)] ³⁺	k_o	1.4×10^{-4}	39(1)	-188(8)		
	k_b	4.2×10^{-5}	115(1)	+59(4)		
	Q_p				65(3)	+238(8)
	k_{OH}^e	4.7×10^{-4}	180	+297		
	k_{aq}	3.9×10^{-5}	77(1)	-71(4)		
[Cr ₂ (tmpa) ₂ (μ -O)(μ -CPh ₃ CO ₂)] ³⁺	k_{aq}	4.9×10^{-6}	96(5)	-25(12)		
[Cr ₂ (tmpa) ₂ (μ -O)(μ -PhCO ₂)] ³⁺	k_{aq}	5.1×10^{-5}	80(1)	-59(4)		
[Cr ₂ (tmpa) ₂ (μ -O)(μ -[Ph-4-NO ₂]CO ₂)] ³⁺	k_{aq}	7.1×10^{-5}	82(1)	-50(4)		

^a See Table 1 for parameter definitions. Standard deviations are shown in parentheses. Conditions for k_o (s⁻¹), k_b (s⁻¹), Q_p (M⁻¹), and k_{OH} (M⁻¹ s⁻¹): $I = 1.0$ M. Conditions for k_{aq} (s⁻¹): $I = 0.1$ M. Enthalpy and entropy changes expressed in kJ mol⁻¹ and J mol⁻¹ K⁻¹, respectively. ^b Parameters from ref 8 pertain to cleavage of first oxo bridge. ^c Parameters from ref 8 pertain to oxo-bridge cleavage. ^d Parameters from ref 9 pertain to rate-limiting loss of both NCS⁻ ligands prior to oxo-bridge cleavage. ^e k_{OH} calculated as $k_b Q_p$; $\Delta H^\ddagger(k_{OH}) = \Delta H^\ddagger(k_b) + \Delta H^\circ(Q_p)$; $\Delta S^\ddagger(k_{OH}) = \Delta S^\ddagger(k_b) + \Delta S^\circ(Q_p)$.

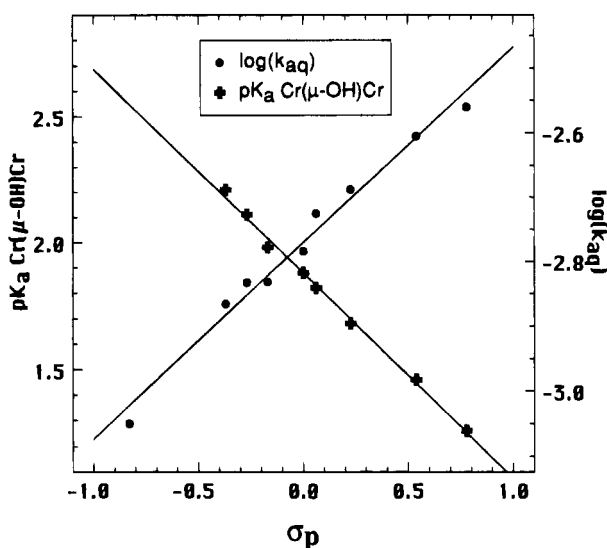


Figure 3. Hammett correlation of aquation rate constants (60.0 °C) and Cr(μ -OH)Cr acid ionization constants (25.0 °C, ref 5) for [(tmpa)Cr(O)([Ph-4-X]CO₂)Cr(tmpa)]³⁺ dimers. $I = 0.1$ M.

than the acid hydrolysis reaction. Such a finding could be reconciled with mechanism 6 provided that the activation barrier for the k_f step is primarily related to Cr-OH₂ bond-making. The failure of $\log(k_o/k_f)$ to correlate with σ_p is inconsistent with mechanism 6, however, as M-OOCR bond-breaking rates are known to be highly sensitive to carboxylate basicity (vide supra). Finally, the solvent-induced carboxylate ring-opening mechanism fails to account for the unique behavior of the formate-bridged dimer. Thus, the unjustifiable assumption that $k_c[OH^-]/k_f \ll 1$ only when R = H is required to account for a first-order OH⁻ dependence in the case of [(tmpa)Cr(O)(HCO₂)Cr(tmpa)]³⁺.

Activation parameters based on k_{aq} for [(tmpa)Cr(O)(HCO₂)Cr(tmpa)]³⁺ acid hydrolysis are essentially identical with those for the k_o base hydrolysis pathway, implying that the two reactions share a common rate-limiting step, unassisted or solvent-assisted ring-opening of the bridging carboxylate ligand. The ring-opening activation barrier of [(tmpa)Cr(O)₂Cr(tmpa)]²⁺ (Table 4) is remarkably similar, in spite of the size and charge

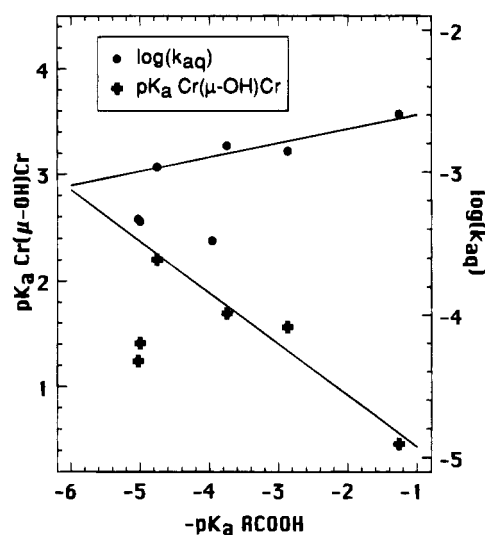


Figure 4. Effect of bridging carboxylate group basicity on aquation rate constants (60.0 °C) and Cr(μ -OH)Cr acid ionization constants (25.0 °C, ref 5) for [(tmpa)Cr(O)(RCO₂)Cr(tmpa)]³⁺ dimers with aliphatic substituents. $I = 0.1$ M. Least-squares lines drawn on the basis of data for R = H, CH₃, CH₂Cl, and CHCl₂ only.

difference between the bridging oxo and formate ligands. This correspondence between ΔH^\ddagger and ΔS^\ddagger values extends to the hydroxide-dependent k_{OH} pathways for cleavage of the dioxo- and oxo, formate-bridged dimers. Thus, both exhibit activation enthalpies on the order of 84 kJ mol⁻¹ and near-zero activation entropies, consistent with direct nucleophilic attack of OH⁻ at Cr(III) accompanied by breaking of the Cr-bridging oxo or formate O bond.

We propose that the [(tmpa)Cr(O)(HCO₂)Cr(tmpa)]³⁺ base hydrolysis mechanism for R \neq H requires preequilibrium displacement of a tmpa pyridyl arm by OH⁻, followed by rate-limiting ring-opening of the bridging carboxylate group assisted by the solvent or migratory, intracomplex nucleophilic attack from the hydroxide ligand (Figure 6). Our rationale for this hypothesis is that steric congestion of the interchromium region by NCS⁻ sulfur atoms of [Cr(tmpa)(NCS)]₂O²⁺, organic substituents of [(tmpa)Cr(O)(RCO₂)Cr(tmpa)]³⁺ dimers and the nonbridging CCl₃CO₂⁻ ligand of [(OH)(tmpa)Cr(μ -O)Cr(tmpa)-

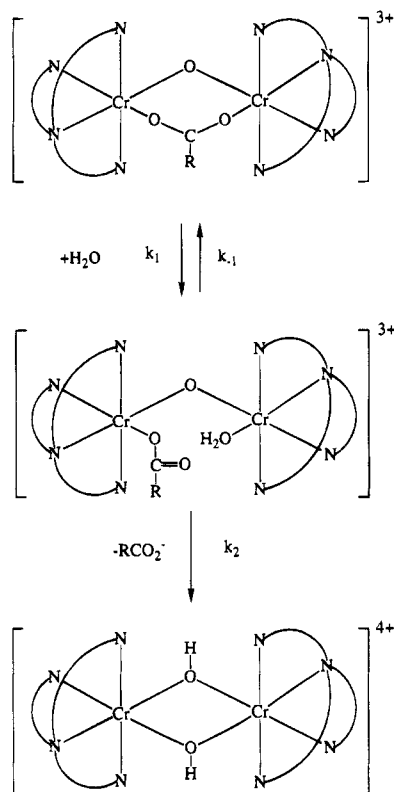


Figure 5. Proposed acid hydrolysis mechanism for $[(\text{tmpa})\text{Cr}(\text{O})(\text{RCO}_2)\text{Cr}(\text{tmpa})]^{3+}$ dimers.

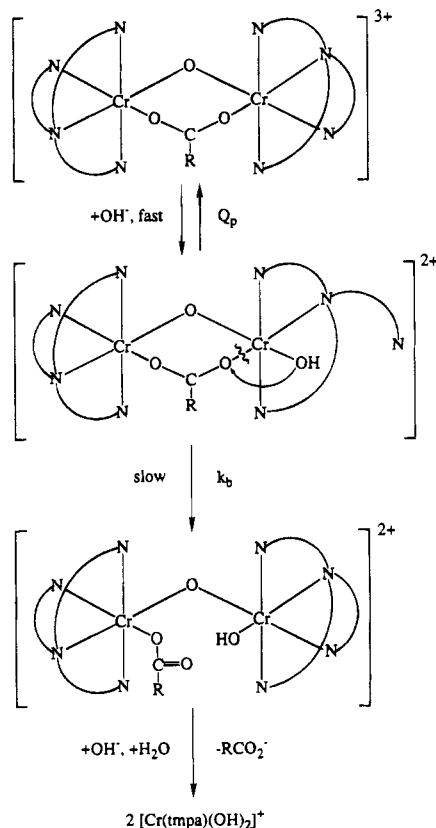


Figure 6. Proposed base hydrolysis mechanism for $[(\text{tmpa})\text{Cr}(\text{O})(\text{RCO}_2)\text{Cr}(\text{tmpa})]^{3+}$ dimers.

$(\text{CCl}_3\text{CO}_2)]^{2+}$ prevents direct nucleophilic attack by OH^- at both the oxo and complementary bridging ligands. Modest lengthenings of the Cr1–N3 (2.087 Å) and Cr2–N7 (2.093 Å) bonds relative to the mean Cr–pyridyl N distance (2.062 Å) were

observed in the crystal structure⁴ of $[(\text{tmpa})\text{Cr}(\text{O})(\text{CH}_3\text{CO}_2)\text{Cr}(\text{tmpa})]^{3+}$, suggesting that one of these bonds is most likely to be cleaved by an incoming hydroxide ligand. While the mechanistic schematic is drawn on the premise that the N3 pyridyl arm, trans to the oxo bridge, is specifically activated, we note that the kinetic data do not require such a conclusion.

In an attempt to detect a pyridyl arm-displaced precursor complex, the 300–450 nm spectrum of $[\text{Cr}_2(\text{tmpa})_2(\text{O})(\text{Ph}_3\text{CCO}_2)]^{3+}$ was measured immediately after mixing with 1.0 M NaOH at 60 °C. The extent of reactant conversion to the proposed pyridyl arm-displaced intermediate should exceed 99% under these conditions on the basis of our kinetically-determined Q_p value. This experiment was inconclusive with regard to the presence of such an intermediate, however, since the positions and relative intensities of reactant charge transfer bands at 337, 371, and 421 nm⁵ were essentially unchanged. Considering the remarkable similarity among electronic spectra of all dimers which contain the $\text{Cr}_2(\mu\text{-O})(\mu\text{-RCO}_2)$ chromophore,^{4,5} our failure to observe distinctively different spectral features for an intermediate which retains this structural feature is not surprising.

The proposed displacement of a tmpa pyridyl arm by OH^- is consistent with the $\Delta H^\circ(Q_p)$ and $\Delta S^\circ(Q_p)$ parameters, which indicate a strongly endothermic process driven by a highly favorable entropy change, presumably linked to both Cr–N bond-breaking and the liberation of solvating water molecules from the reactants. The precursor formation constant Q_p is remarkably insensitive to the nature of the R group, falling within the narrow 71–230 M⁻¹ interval for 13 of the 15 bridging carboxylate ligands examined, including both aliphatic and aromatic substituents. The only exceptions (R = CHCl_2 , and Ph-4-O^-) are dimers for which atypically small Q_p values coincide with exceptionally large k_o parameters. Thus, the hydroxide-independent pathway becomes more prominent as hydroxide-dimer complexation weakens. The failure of Q_p to correlate with carboxylate inductive characteristics is expected, as the thermodynamics of remote chromium–pyridyl N bond-breaking should be little affected by variations in a bridging ligand substituent.

Although the largest (R = CHCl_2) and smallest (R = CPh_3) k_b rate constants are associated with particularly low and high Q_p values, respectively, there is not a consistent trend in this direction when all of the data is considered. A plot of k_b vs k_{aq} shows that substituents which cause steric retardation of acid hydrolysis (R = $\text{C}(\text{CH}_3)_3$, CPh_3 , 1-adamantyl) also impede base hydrolysis, although to a lesser extent, while the second-most reactive bridging carboxylate toward aquation (R = CHCl_2) remains exceptionally labile under basic conditions. Curiously, the high relative reactivity of the *p*-nitrobenzoato complex in acidic media is largely damped in the base hydrolysis reaction. The average k_b/k_{aq} ratio (6.7 ± 2.3) denotes a moderate degree of carboxylate ring-opening activation in the base hydrolysis intermediate. Considering also the extraordinarily small reaction constant for base hydrolyses of 4-XPhCO₂⁻ bridging ligands, we conclude that the extent of Cr–carboxylate O bond-breaking in the rate-limiting step is attenuated relative to the k_1 process for aquation.

The temperature dependence of k_b for R = CH_3 makes it clear that the rate-limiting step is promoted by a positive ΔS^\ddagger which offsets an unexpectedly high enthalpic activation barrier. Thus, ΔH^\ddagger and ΔS^\ddagger values for the k_b pathway are 38 kJ mol⁻¹ and 130 J mol⁻¹ K⁻¹ more positive, respectively, than the corresponding k_{aq} activation parameters. While the favorable entropic term may be understood in part by the enablement of rotation about the Cr–O–Cr and Cr–O₂CR bond axes upon

displacement of a carboxylate bridge, the factors underlying such a large increase in ΔH^\ddagger are less clear, particularly since charge reduction¹⁰ at the Cr center ligated by OH⁻ should promote cleavage of the bond between this chromium atom and the bridging carboxylato ligand. We note that the activation enthalpies for OH⁻-dependent hydrolysis pathways substantially exceed those of the corresponding k_o terms for all dimers in this class examined to date, including [Cr(tmpa)(O)]₂²⁺, [Cr(tmpa)L]₂O²⁺ (L = NCS⁻, OH⁻) and [(tmpa)Cr(O)(RCO₂)Cr(tmpa)]³⁺ (R = H, CH₃). In the latter case, the enhancement in ΔH^\ddagger could reflect an energetic cost associated with hydroxo or oxo ligand migration^{1,9,26} required to initiate carboxylate ring-

opening. Unlike the formate-bridged dimer, [(tmpa)Cr(μ -O)(μ -CH₃CO₂)Cr(tmpa)]³⁺ exhibits very different activation parameters for k_{aq} and k_o hydrolysis pathways; in the latter instance, ΔH^\ddagger is smaller by 38 kJ mol⁻¹ while ΔS^\ddagger is more negative by 117 J mol⁻¹ K⁻¹. Kinetically-indistinguishable alternatives which should be considered for this distinctive k_o pathway include solvent-assisted processes such as oxo-bridge cleavage or carboxylate C-O bond-breaking.

Acknowledgment. We thank the Welch Foundation (Grant D-735) for support of this research.